Ther Adv Hematol

2020, Vol. 11: 1–12

DOI: 10.1177/2040620720932686

BRD4 inhibitor nitroxoline enhances the sensitivity of multiple myeloma cells to bortezomib *in vitro* and *in vivo* by promoting mitochondrial pathway-mediated cell apoptosis

Guang Li*, Yan-Hua Zheng*, Li Xu, Juan Feng, Hai-Long Tang, Cheng Luo, Yan-Ping Song and Xie-Qun Chen

Abstract

Background: Multiple myeloma (MM) is the second most common hematological neoplasm. Wide administration of bortezomib significantly improves the survival of MM patients compared with conventional chemotherapy. Bromodomain-containing protein 4 (BRD4) inhibitors also have been demonstrated to retard cell proliferation and induce cellular apoptosis in various cancers. However, it is unclear whether the BRD4 inhibitor nitroxoline plus bortezomib has a synergistic anti-tumor effect on MM.

Methods: Cell viability was determined *via* 3-(4,5-Dimethylthiazol-2-yl)-2,5-diphenyltetrazolium bromide (MTT) assay. Cell cycle and cell apoptosis were assessed *via* flow cytometry. Protein expression levels were determined *via* western blotting. The expression of apoptosis-related proteins in xenograft tissue were detected by means of immunohistochemistry.

Results: Treatment with nitroxoline or bortezomib suppressed cell proliferation, and caused G0/G1 phase arrest and apoptosis in H929 and RPMI8226 cells. Furthermore, nitroxoline intensified the retardation of cell proliferation, as well as further enhanced the G0/G1 phase arrest and apoptosis induced by bortezomib in H929 and RPMI8226 cells. The western blot analysis revealed that nitroxoline or bortezomib treatment markedly diminished the levels of Bcl-2 and cyclin D1, and increased the levels of p21, Bax, cleaved PARP and cleaved caspase-3. Combination of these two agents was observed to result in further marked changes on these levels compared with nitroxoline or bortezomib treatment alone. What is more, in the xenograft tumor model, combinative treatment markedly inhibited tumor growth compared with the single drug treatment.

Conclusion: Combination of bortezomib with nitroxoline has a synergistic anti-tumor activity in MM cells and may be a novel treatment method for MM.

Keywords: apoptosis, BRD4 inhibitor, G1 phase cell cycle checkpoint, multiple myeloma

Received: 4 February 2020; revised manuscript accepted: 15 May 2020.

Correspondence to:
Xie-Qun Chen
Department of Hematology, Xijing Hospital, Fourth Military Medical University, 127 Changle West Road, Xi'an, Shaanxi 710032, P.R. China
xiequnchen1@163.com

Yan-Ping Song
Institute of Hematology, Xi'an Central Hospital, 161 Xiwu Road, Xi'an, Shaanxi 710003, P.R. China
xjtusyp123@163.com

Guang Li
Department of Hematology, Xijing Hospital, Fourth Military Medical University, Xi'an, Shaanxi, China

Institute of Hematology, Xi'an Central Hospital, Xi'an, Shaanxi, China

Yan-Hua Zheng
Li Xu
Juan Feng
Hai-Long Tang
Department of Hematology, Xijing Hospital, Fourth Military Medical University, Xi'an, Shaanxi, China

Cheng Luo
State Key Laboratory of Drug Research, Drug Discovery and Design Center, Shanghai Institute of Materia Medica, Chinese Academy of Science, Shanghai, China

*Guang Li and Yan-Hua Zheng contributed equally to this article as co-first authors.

Introduction

Multiple myeloma (MM), the second most common hematological neoplasm, is characterized by clonal proliferation of plasma cells within the bone marrow.[1,2] During the past decades, proteasomes have been tested as a new effective target in the treatment of MM[3] and the first-generation proteasome inhibitor bortezomib significantly improved therapeutic effect compared with previously used treatments.[4,5] In addition, novel agents including monoclonal antibodies and histone deacetylase inhibitors have also been used to treat

MM, resulting in significant extension of patients' survival.[6] Bortezomib remains the mainstay of MM treatment and bortezomib resistance is unavoidable.[7,8] Therefore, it is imperative to develop more efficient strategies to augment the sensitivity of bortezomib and reverse drug resistance.

The bromodomain-containing protein 4 (BRD4) is the most studied member of the bromodomain and extraterminal domain (BET) protein family, which can recognize acetylated-histones and activate downstream gene expression *via* recruiting transcription factors.[9,10] Previous studies have demonstrated that deregulation of the BRD4 protein took an important part in tumorigenesis, including in the development of prostate, colorectal, pancreatic, lung and breast cancer. And BRD4 inhibitors, such as JQ1, SF1126 and SF2523, have been demonstrated to exert an anti-tumor effect on various types of tumors.[11–13] Furthermore, Guo *et al.*[14] demonstrated that the BET inhibitor I-BET151 had a beneficial effect in MM treatment by inhibiting the BRD4-mediated signaling pathway. In addition, Jiang *et al.*[15] reported that nitroxoline acted as a BRD4 inhibitor. However, the pharmacological effects of nitroxoline in MM remain unclear.

Our study aimed to explore the synergistic effects of nitroxoline and bortezomib on cell proliferation, cell cycle progression and apoptosis in MM. We also investigated the molecular mechanism by which nitroxoline and bortezomib combated against MM. The combination of nitroxoline with bortezomib may be a novel treatment for MM.

Material and methods

Reagents and antibodies

3-(4,5-Dimethylthiazol-2-yl)-2,5-diphenyltetrazolium bromide (MTT) was purchased from Sigma Aldrich (Merck KGaA) Nitroxoline was kindly provided by Dr Cheng Luo as a gift, while bortezomib was obtained as a pure substance from Millennium Pharmaceuticals. Antibodies against B-cell lymphoma 2 (Bcl-2) (ab182858), Bcl-2-associated X protein (Bax) (ab32503), cleaved poly (ADP-ribose) polymerase (PARP) (ab74290), cyclin D1 (ab134175), p21 (ab109199) and GAPDH (ab128915) were obtained from Abcam, while the antibody against cleaved caspase-3 (cat. no. 9664), anti-rabbit HRP secondary antibody (cat. no. 7074) was purchased from Cell Signaling Technology, Inc. RPMI 1640 medium and fetal bovine serum (FBS) were purchased from Thermo Fisher Scientific, Inc. (Gibco).

Cell culture and treatments

The human MM cell lines H929 and RPMI8226 (American Type Culture Collection) were cultured in RPMI-1640 medium supplemented with 10% FBS, 100 U/ml penicillin and 100 μg/ml streptomycin at 37°C with 5% CO2.

RPMI8226 and H929 cells were treated with 0, 0.25, 0.50, 1.00, 2.00, 4.00, 8.00 and 16.00 μM nitroxoline for 24 h, and the cell viability was determined *via* MTT assay. Subsequently, RPMI8226 cells were treated with 0, 1, 2, 4, 8, 16, 32 and 64 nM bortezomib, H929 cells were treated with 0, 0.125, 0.25, 0.5, 1, 2, 4 and 8 nM bortezomib for 24 h, and then cell viability was determined *via* an MTT assay. Dimethyl sulfoxide (DMSO) was used in the control group at the same dilution as the corresponding treatment in the nitroxoline and bortezomib alone groups. Finally, RPMI8226 cells were treated with 0.5 μM nitroxoline and 5.0 nM bortezomib for 24 h, while H929 cells were treated with 0.25 μM nitroxoline and 1.00 nM bortezomib for 24 h, and then the cell cycle distribution and cell apoptosis were examined *via* flow cytometry.

MTT cytotoxicity assay

Cell viability was measured using an MTT assay. Briefly, the H929 and RPMI8226 cells were seeded into 96 well plates at a density of 1.5×10^4 cells/well for 12 h. Next, the cells were treated with different concentrations of nitroxoline and bortezomib for 24 h. A final concentration of 0.5 mg/ml MTT was then added to each well and incubated for an additional 4 h at 37°C. Cells were adhered to a 96-well plate *via* centrifugation at 2000 *g* for 10 min at 25°C. The supernatant was then discarded after centrifugation, and 150 μl/well DMSO (Sigma Aldrich; Merck KGaA) was added to dissolve the solid residue. Finally, the absorbance at 570 nm was determined using a microplate reader (DNM 9602; Perlong Medical Equipment Co., Ltd.). All experiments were performed at least in triplicate.

Cell cycle assay

For the assessment of cell cycle progression, the H929 and RPMI8226 cells were seeded at a density of 2.5×10^5 cells/ml in six-well plates, and treated with different concentrations of nitroxoline and/or bortezomib for 24 h. Next, the H929 and RPMI8226 cells were fixed with 75% ethanol overnight. Propidium iodide (PI; Sigma-Aldrich; Merck KGaA) was then used to stain the DNA of samples for 15 min. Subsequently, flow cytometry was conducted with an Epics XL flow cytometer (Beckman Coulter, Inc.) to determine the cell cycle progression, and data were analyzed using Flowjo software (version 7.6; FlowJo, LLC). All experiments were performed at least in triplicate.

Apoptosis assay

The H929 and RPMI8226 cells were seeded at a density of 2.5×10^5 cells/ml in six-well plates, and treated with different concentrations of nitroxoline and/or bortezomib for 24 h. Cell apoptosis was then assessed using an Annexin V-fluorescein isothiocyanate (FITC) Apoptosis Detection kit (BD Biosciences). Briefly, the cells were stained with Annexin V-FITC and PI in binding buffer for 15 min, and the apoptotic cells were then detected using a FACScalibur flow cytometer (BD Biosciences). The results were analyzed using CXP software (version 2.1; Beckman Coulter, Inc.). All experiments were performed at least in triplicate.

Western blotting

Following the different treatments, the cells were lysed in lysis buffer as previously described,[16,17] and then the cell lysates were separated *via* SDS-PAGE (10–18% gel). Proteins were transferred onto nitrocellulose membranes (Pall Corporation), and the membranes were then blocked with 5% non-fat milk in Tris-buffered saline/Tween 20 (consisting of 50 mM Tris-HCl, pH 8.0, 10 mM NaCl and 0.1% Tween 20) for 2 h at room temperature. Subsequently, the membranes were incubated overnight at 4°C with anti-cyclin D1(dilution 1:3000), anti-p21 (dilution 1:1000), anti-Bax (dilution 1:1000), anti-Bcl2 (dilution 1:1000), anti-cleaved caspase-3 (dilution 1:500), anti-cleaved PARP (dilution 1:1000) and anti-GAPDH (dilution 1:3000) primary antibodies. The membranes were then incubated with anti-rabbit HRP secondary antibody (1:20,000, cat. no. 7074, Cell Signaling Technology, Inc.) for 2 h at 25°C. Visualization was achieved using SuperSignal West Pico chemiluminescent Substrate (Pierce; Thermo Fisher Scientific, Inc.) and Aplegen (Omega Lum G).

In vivo *human plasmacytoma xenograft model*

All experimental protocols were approved by Animal Ethics Committee of The First Affiliated Hospital of the Fourth Military Medical University (No. IACUC-20160905).

A xenograft tumor model was established as previously described.[18] Briefly, 24 female BALB/c nude mice (16–20 g; 4–6 weeks) were obtained from Shanghai Laboratory Animal Center. Female BALB/c nude mice were housed at 22 ± 2°C room with a 12-h light/12-h dark cycle, a relative humidity of 40–60%, and had free access to food and water. RPMI8226 cells (1×10^7 per mouse) were injected subcutaneously into the right flanks of nude mice in 100 µl serum-free RPMI-1640 medium. Seven days after tumor cell injection, the mice were divided into four groups ($n = 3$ per group), as follows: saline control, bortezomib (0.6 mg/kg) or nitroxoline (60 mg/kg) treatment alone, and combination of bortezomib (0.6 mg/kg) and nitroxoline (60 mg/kg) treatment groups. Nitroxoline (60 mg/kg) was administered *via* intraperitoneal injection three times per 7 days, while bortezomib (0.6 mg/kg) was administered *via* intravenous injection twice per 7 days for 14 days. The volume of the tumor was measured every 3 days for 21 days and was calculated as follows: Volume (mm^3) = (long diameter of the tumor) × (short diameter of the tumor)^2/2. At the end of the experiment (day 21), the mice underwent euthanasia *via* CO_2 asphyxiation in a chamber (100% CO2, 9.6 l/min, 10 min) followed by cervical dislocation to confirm death, and the tumors were excised. The tumor samples were then examined using hematoxylin and eosin (HE) staining. Furthermore, a TUNEL assay was performed to detect *in situ* apoptosis using a *In Situ* Cell Death Detection Kit, POD (cat. no. 11684817910, Roche, USA) according to the manufacturer's instructions and immunohistochemical staining was used to assess the Ki-67 expression of tumor tissues using a Ki-67 assay kit (immunohistochemical) (cat. no. MAB-0672, MXB Biotechnology, Fuzhou, China) according to the manufacturer's

instructions for quantifying the cell proliferation in the human plasmacytoma xenograft model. All procedures were carried out in accordance with the Guide for the Care and Use of Laboratory Animals published by the US National Institutes of Health (NIH publication No. 85-23, revised 1996).

Statistical analysis

The results are presented as the mean ± standard deviation. One-way analysis of variance followed by Dunnett's and Tukey's *post-hoc* tests were used to determine the statistical significance of the observed differences, with $p < 0.05$ considered statistically significance.

Results

Nitroxoline increases the bortezomib-induced proliferation inhibition in human MM cell lines

In order to investigate the effect of nitroxoline and bortezomib on human MM cell proliferation, H929 and RPMI8226 cells were treated with different concentrations of bortezomib and nitroxoline for 24 h, and cell viability was investigated using an MTT assay. As presented in Figure 1(A) and (B), bortezomib or nitroxoline as single treatments significantly inhibited the viability of H929 and RPMI8226 cells compared with the control group, in a concentration-dependent manner. The viability of cells co-treated with bortezomib and nitroxoline was further measured. As presented in Figure 1(C), 5.00 nM bortezomib and 0.50 nitroxoline combination was able to markedly inhibit the viability RPMI8226 cells, 1.00 nM bortezomib and 0.25 nitroxoline combination was able to markedly inhibit the viability of H929 in comparison with that in the bortezomib or nitroxoline single treatment groups. These results indicated that nitroxoline was able to increase the sensitivity of H929 and RPMI8226 cells to bortezomib, contributing to the suppression of cell proliferation.

Nitroxoline increases the bortezomib-induced G0/G1 phase arrest in human MM cell lines

The present study further investigated the effects of nitroxoline and bortezomib on the cell cycle progression of human MM cells. H929 and RPMI8226 cells were treated with bortezomib and/or nitroxoline for 24 h, and the cell cycle distribution was determined *via* flow cytometry. It was revealed that bortezomib or nitroxoline treatment significantly induced G0/G1 phase cell cycle arrest in H929 and RPMI8226 cells. Furthermore, the combination of bortezomib and nitroxoline significantly increased the G0/G1 phase cell cycle arrest compared with the H929 and RPMI8226 cells treated with bortezomib or nitroxoline alone (Figure 2(A) and (B)). Our data suggested that nitroxoline significantly increased the bortezomib-mediated G0/G1 phase arrest in H929 and RPMI8226 cells.

Effect of nitroxoline and bortezomib on cell cycle-associated protein in human MM cell lines

In order to further elucidate the mechanism underlying the G0/G1 phase arrest, the present study detected the expression levels of cyclin D1 and p21 in H929 and RPMI8226 cells. As presented in Figure 3(A), nitroxoline evidently decreased the level of cyclin D1 and increased the level of p21 in a concentration-dependent manner. In addition, the combination of bortezomib and nitroxoline clearly decreased the level of cyclin D1 and increased the level of p21 compared with those in the bortezomib or nitroxoline alone groups (Figure 3(B)). These results suggested that nitroxoline significantly increased the bortezomib-mediated G0/G1 phase arrest *via* downregulating the expression of cyclin D1 protein and upregulating the expression of p21 protein in H929 and RPMI8226 cells.

Nitroxoline increases the bortezomib-induced apoptosis in human MM cell lines

The present study further investigated the effect of nitroxoline and bortezomib on human MM cell apoptosis. H929 and RPMI8226 cells were treated with bortezomib and/or nitroxoline for 24 h, and then cell apoptosis was investigated using flow cytometry. As presented in Figure 4(A) and (B), bortezomib and nitroxoline induced apoptosis in H929 and RPMI8226 cells. Furthermore, the combination of bortezomib and nitroxoline significantly increased the percentage of apoptotic cells compared with the bortezomib or nitroxoline alone groups. These results indicated that nitroxoline may significantly increase bortezomib-induced cell apoptosis.

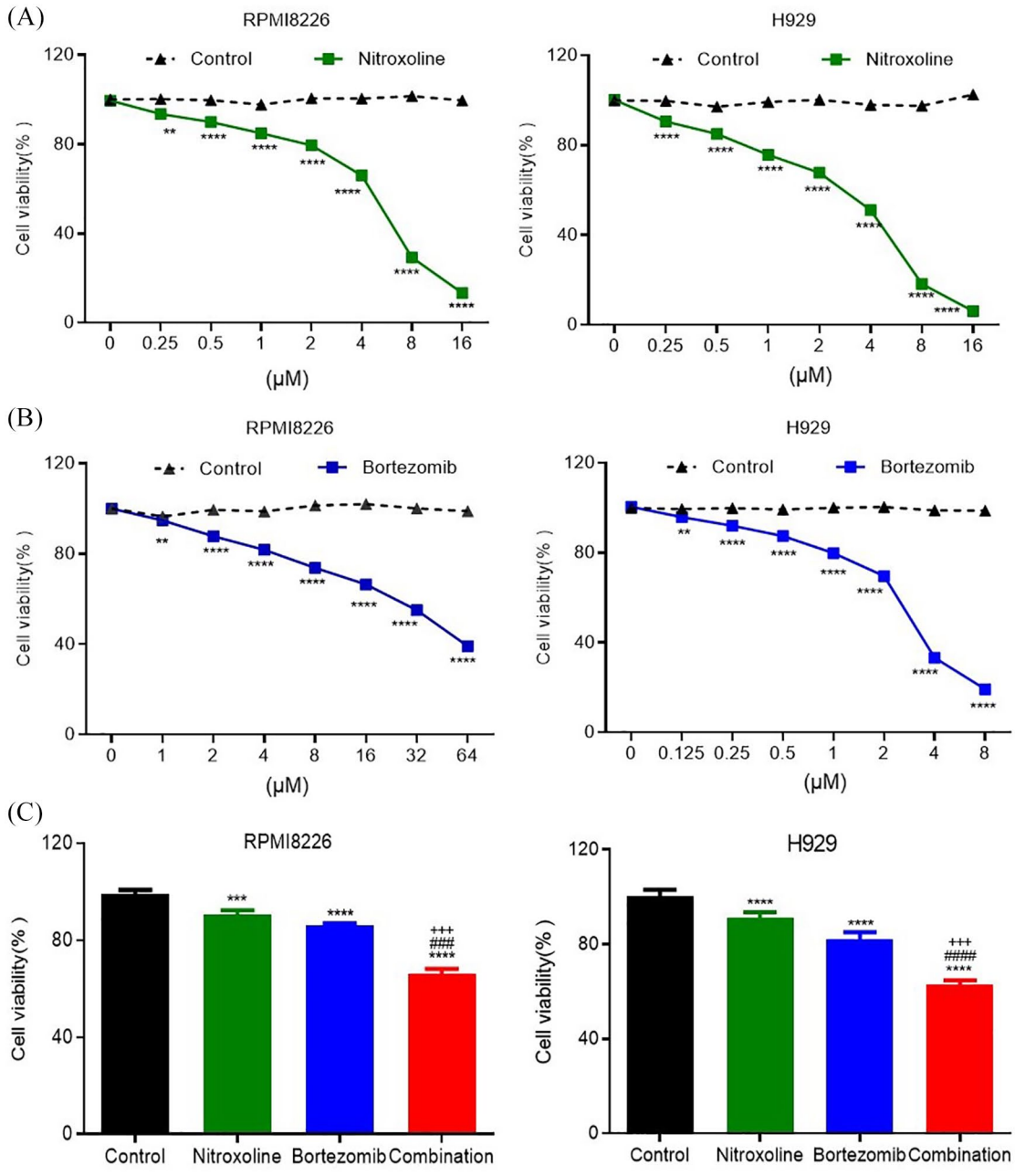

Figure 1. Effects of nitroxoline and bortezomib on the proliferation of RPMI8226 and H929 cells. (A) RPMI8226 and H929 cells were treated with various concentrations of nitroxoline (0.00, 0.25, 0.50, 1.00, 2.00, 4.00, 8.00 and 16.00 μM) for 24 h, and the cell viability was determined *via* MTT assay. (B) Cells were treated with various concentrations of bortezomib (RPMI8226 cells: 0, 1, 2, 4, 8, 16, 32 and 64 nM; H929 cells: 0, 0.125, 0.25, 0.5, 1, 2, 4 and 8 nM) for 24 h, and then cell viability was determined *via* an MTT assay. DMSO was used in the control group at the same dilution as the corresponding treatment in the nitroxoline and bortezomib alone group. (C) Cells were treated with nitroxoline and/or bortezomib for 24 h (RPMI8226 cells, 0.50 μM and 5.00 nM, respectively; H929 cells, 0.25 μM and 1.00 nM, respectively), and cell viability was determined *via* an MTT assay. Data are presented as the mean ± standard deviation from three independent experiments. (**$p < 0.01$, ***$p < 0.001$ and ****$p < 0.0001$, *versus* control group; ###$p < 0.001$ and ####$p < 0.0001$ *versus* nitroxoline alone group; $^{+++}p < 0.001$ *versus* bortezomib alone group.)

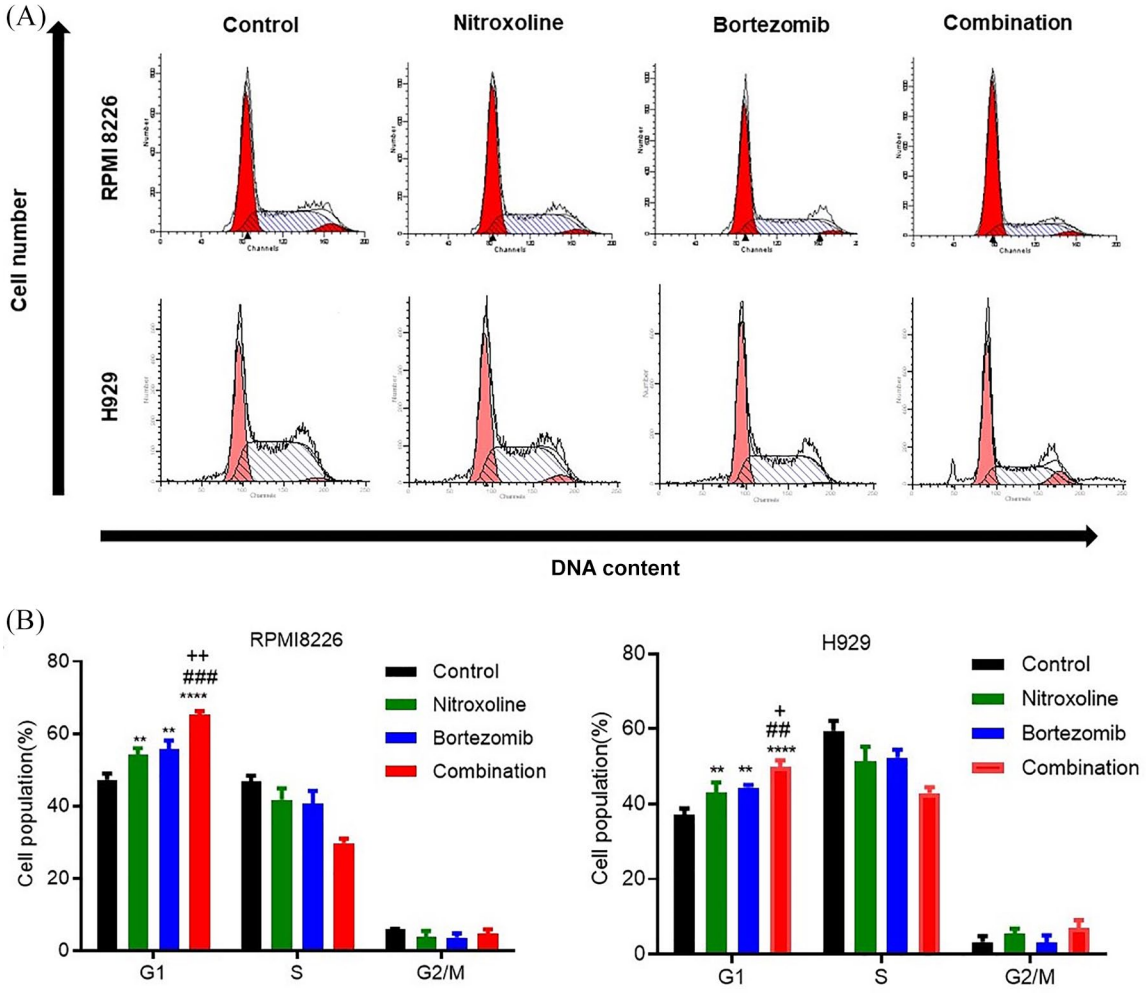

Figure 2. Effects of nitroxoline and bortezomib on cell cycle distribution in RPMI8226 and H929 cells. (A) RPMI8226 cells were treated with 0.5 μM nitroxoline and 5.0 nM bortezomib for 24 h, while H929 cells were treated with 0.25 μM nitroxoline and 1.00 nM bortezomib for 24 h. Next, the cell cycle distribution was examined *via* flow cytometry. (B) Quantification of the cell cycle distribution. (**$p < 0.01$, ****$p < 0.0001$, *versus* control group; ##$p < 0.01$, ###$p < 0.001$, *versus* nitroxoline alone group; +$p < 0.05$ and ++$p < 0.01$, *versus* bortezomib alone group.)

Effect of nitroxoline and bortezomib on apoptosis-associated protein in human MM cell lines

In addition, a number of apoptosis-associated proteins in H929 and RPMI8226 cells were detected *via* western blotting. As presented in Figure 5(A), nitroxoline evidently decreased the level of Bcl-2, and increased the levels of Bax, cleaved PARP and cleaved caspase-3 in a concentration-dependent manner. The combination of bortezomib and nitroxoline markedly decreased the level of Bcl-2, and increased the levels of Bax, cleaved PARP and cleaved caspase-3, as compared with those in the bortezomib or nitroxoline alone groups (Figure 5(B)). Overall, these results demonstrated that nitroxoline may significantly increase the cell apoptosis induced by bortezomib *via* mitochondrial-dependent apoptotic pathways.

Nitroxoline enhances the bortezomib-induced inhibition of xenograft tumor growth in mice in vivo

The present study next investigated the effects of nitroxoline and bortezomib on RPMI8226 cell

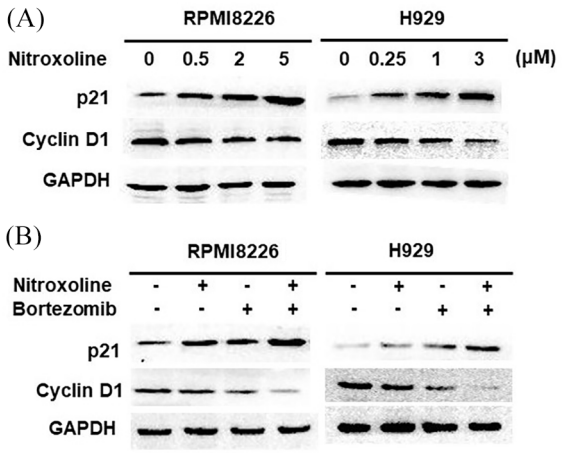

Figure 3. Effects of nitroxoline and bortezomib on cell cycle-related protein in RPMI8226 and H929 cells. (A) RPMI8226 cells were treated with 0, 0.5, 2, 5 μM nitroxoline for 24 h, H929 cells were treated with 0, 0.25, 1, 3 μM nitroxoline for 24 h. Cyclin D1 and p21 protein expression levels were examined *via* western blotting. (B) Cyclin D1 and p21 protein expression levels were examined *via* western blotting in RPMI8226 cells treated with 0.5 μM nitroxoline and 5.0 nM bortezomib for 24 h, and in H929 cells treated with 0.25 μM nitroxoline and 1.00 nM bortezomib for 24 h. GAPDH was used as the internal control in western blotting experiments.

tumor growth in a subcutaneous tumor model in mice. The nude mice were randomly assigned into four groups (three mice per group), and treated with bortezomib (0.6 mg/kg) and/or nitroxoline (60 mg/kg) for 14 days. As presented in Figure 6(A), the tumor growth was markedly inhibited by bortezomib or nitroxoline treatment. Compared with the single treatment groups, the combination treatment markedly inhibited the tumor growth (Figure 6(A)). As presented in Figure 6(B), HE staining revealed that the combination of bortezomib and nitroxoline increased the cell apoptosis observed in the tumor tissue as compared with the control group (Figure 6(B)). Ki-67 positive cells shrank in tumor sections from mice treated with bortezomib and nitroxoline (Figure 6(B)). Furthermore, the combination of bortezomib and nitroxoline remarkably increased the number of TUNEL-positive cells in comparison with each treatment alone group (Figure 6(C)). These results demonstrated that nitroxoline magnified the anti-cancer effect of bortezomib against MM cells *in vivo*.

Discussion

Nitroxoline, a urinary antibacterial agent, has also been regarded as a selective BET inhibitor, which noticeably disrupts the binding between BRD4_BD1 and acetylated H4, and inhibits all BET proteins with approximately 20-fold selectivity against other non-BET bromodomain-containing proteins.[15] The present study aimed to investigate the effect of nitroxoline on the bortezomib-induced death of RPMI8226 and H929 cells. The results verified that the combination of bortezomib and nitroxoline enhanced the inhibition of proliferation, and enhanced G0/G1 phase cell cycle arrest and apoptosis in H929 and RPMI8226 cells compared with that in cells treated with a single drug or untreated cells. In addition, it was observed that nitroxoline enhanced the bortezomib-induced G0/G1 arrest by downregulating the expression of cyclin D1 protein and upregulating the expression of p21 protein in the cells. The data also indicated that nitroxoline may enhance bortezomib-induced cell apoptosis *via* activating the mitochondrial-dependent apoptotic pathway in H929 and RPMI8226 cells. Furthermore, *in vivo* experiments performed in the present study demonstrated that combination treatment remarkably inhibited the tumor growth and induced cell apoptosis in comparison with the use of single drug treatment in an RPMI8226 xenograft tumor model.

The disorder of the cell cycle is usually a characteristic of human tumors. Thus, cell cycle arrest plays an active role in cell proliferation inhibition caused by anti-cancer drugs.[17,19–21] A number of studies have reported that bortezomib may induce cell cycle arrest in various types of tumor cells lines, including colon cancer,[22] ovarian cancer[23] and MM cells.[24] Furthermore, indole-3-carbinol has been demonstrated to enhance the bortezomib-induced G2/M phase arrest in OVCAR3 and OVCAR5 cells.[25] In HT29 and HCT116 cells, the combination of vorinostat and bortezomib induced G2/M phase arrest.[26] The results of the present study demonstrated that treatment with nitroxoline or bortezomib shifted the cell cycle towards G0/G1 phase in H929 and RPMI8226 cells, as observed *via* flow cytometric analysis. The combination of bortezomib and nitroxoline significantly increased G0/G1 phase cell cycle arrest as compared with the bortezomib or nitroxoline alone

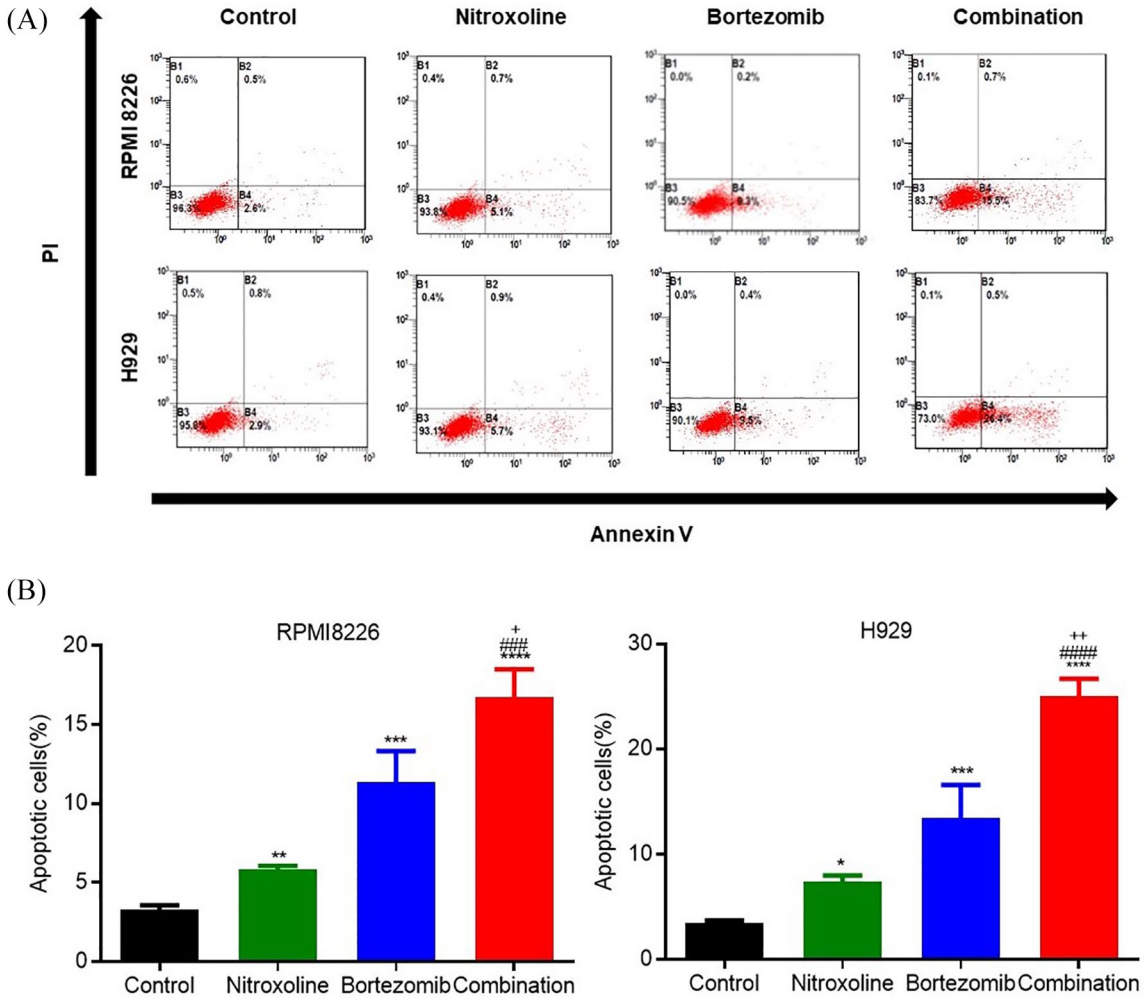

Figure 4. Effects of nitroxoline and bortezomib on the apoptosis of H929 and RPMI8226 cells. (A) Apoptosis was assessed *via* flow cytometry in RPMI8226 cells treated with 0.5 μM nitroxoline and 5.0 nM bortezomib for 24 h, and H929 cells treated with 0.25 μM nitroxoline and 1.00 nM bortezomib for 24 h. (B) Percentage of apoptotic cells. ($^{*}p < 0.05$, $^{**}p < 0.01$, $^{***}p < 0.001$ and $^{****}p < 0.0001$, *versus* control group; $^{\#\#\#}p < 0.001$, $^{\#\#\#\#}p < 0.0001$, *versus* nitroxoline alone group; $^{+}p < 0.05$, $^{++}p < 0.01$, *versus* bortezomib alone group.) PI, propidium iodide

groups. It has been reported that the transition from G0/G1 to S phase is regulated by cyclin D1 and p21 proteins.[27–29] In order to further investigate the molecular mechanism underlying the G0/G1 phase cell cycle arrest induced by nitroxoline and bortezomib in H929 and RPMI8226 cells, the present study assessed the expression levels of cyclin D1 and p21 proteins. The data revealed that nitroxoline markedly decreased the level of cyclin D1 and increased the level of p21 in a concentration-dependent manner. In addition, the combination of bortezomib and nitroxoline markedly decreased the level of cyclin D1 and increased the level of p21 when compared with the bortezomib or nitroxoline alone groups. These findings provided evidence that the addition of nitroxoline enhanced the bortezomib-induced inhibition of H929 and RPMI8226 cell proliferation, through inducing G0/G1 phase arrest *via* downregulating the expression of cyclin D1 protein and upregulating the expression of p21 protein.

Apoptosis has a balancing role in cell proliferation and cell death. Previous studies have reported that the majority of drugs exert their

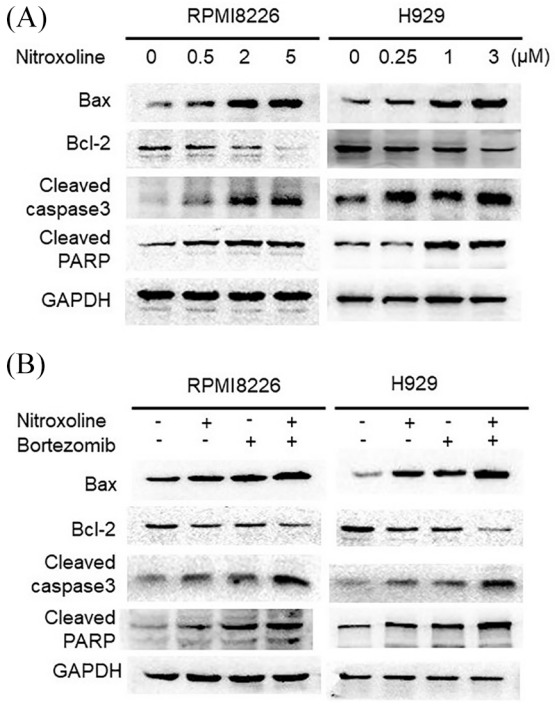

Figure 5. Effects of nitroxoline and bortezomib on apoptosis-related protein of H929 and RPMI8226 cells. (A) RPMI8226 cells were treated with 0, 0.5, 2, 5 μM nitroxoline for 24 h, H929 cells were treated with 0, 0.25, 1, 3 μM nitroxoline for 24 h. Bcl-2, Bax, cleaved PARP and cleaved caspase-3 protein expression levels were assessed *via* western blotting. (B) Bcl-2, Bax, cleaved PARP and cleaved caspase-3 protein expression levels were assessed *via* western blotting in RPMI8226 cells treated with 0.5 μM nitroxoline and 5.0 nM bortezomib for 24 h, and in H929 cells treated with 0.25 μM nitroxoline and 1.00 nM bortezomib for 24 h. GAPDH was used as the internal control. Bax, Bcl-2-associated X protein; BcL-2, B-cell lymphoma 2; PARP, poly (ADP-ribose) polymerase

anti-cancer effects *via* inducing apoptosis of tumor cells.[28,30,31] In addition, Zhang *et al.*[32] revealed that bortezomib triggered cell apoptosis in cervical cancer cells. Bruning *et al.*[23] further reported that bortezomib also triggered apoptosis in ovarian cancer cells. The present study revealed that bortezomib or nitroxoline significantly induced the apoptosis of H929 and RPMI8226 cells. The combination of bortezomib and nitroxoline significantly increased the percentage of apoptotic cells compared with the bortezomib or nitroxoline alone groups. Furthermore, it is well known that apoptosis of tumor cells is often induced by anti-cancer drugs through the mitochondrial pathway.[33–35] Previous studies have confirmed that caspases and Bcl-2 family proteins, such as Bax and Bcl-2, serve important roles in the mitochondrial apoptotic pathway.[36–38] Mortenson *et al.*[39] demonstrated that bortezomib triggered cell apoptosis in small cell lung cancer *via* decreasing Bcl-2 levels. The results of the present study revealed that nitroxoline markedly decreased the level of Bcl-2, and increased the levels of Bax, cleaved PARP and cleaved caspase-3 in a concentration-dependent manner in H929 and RPMI8226 cells. It was further observed that the combination of bortezomib and nitroxoline markedly decreased the level of Bcl-2, and increased the levels of Bax, cleaved PARP and cleaved caspase-3 compared with the bortezomib or nitroxoline alone groups in H929 and RPMI8226 cells. These results suggested that nitroxoline may enhance the bortezomib-induced apoptosis of H929 and RPMI8226 cells through the mitochondrial-dependent apoptotic pathway.

In conclusion, the results of the present study verified that nitroxoline augmented the hindrance of cell proliferation, and strengthened the G0/G1 phase cell cycle arrest and apoptosis induced by bortezomib in H929 and RPMI8226 cells. Furthermore, nitroxoline was observed to enhance the bortezomib-induced G0/G1 arrest *via* downregulating cyclin D1 protein expression and upregulating p21 protein expression. The data also indicated that nitroxoline may enhance the bortezomib-induced cell apoptosis *via* the mitochondrial apoptotic pathway. Importantly, the dose of nitroxoline and bortezomib used *in vitro* is achievable clinically because the concentration of the combination of nitroxoline and bortezomib used in H929 and RPMI8226 did not exceed blood drug peak concentration in patients' clinical application.[40,41] However, there is a limitation in our present study. The dosages of nitroxoline and bortezomib *in vivo* are higher than those which have been readily implemented in clinical treatment and our study lacked the evaluation of adverse drug reactions. But nitroxoline cotreatment with bortezomib did not result in additional toxicity in treated animals. We have confirmed that nitroxoline as BRD4 inhibitor could enhance the sensitivity of bortezomib in multiple myeloma cells. Therefore, it provides the basis for the combinative administration of bortezomib

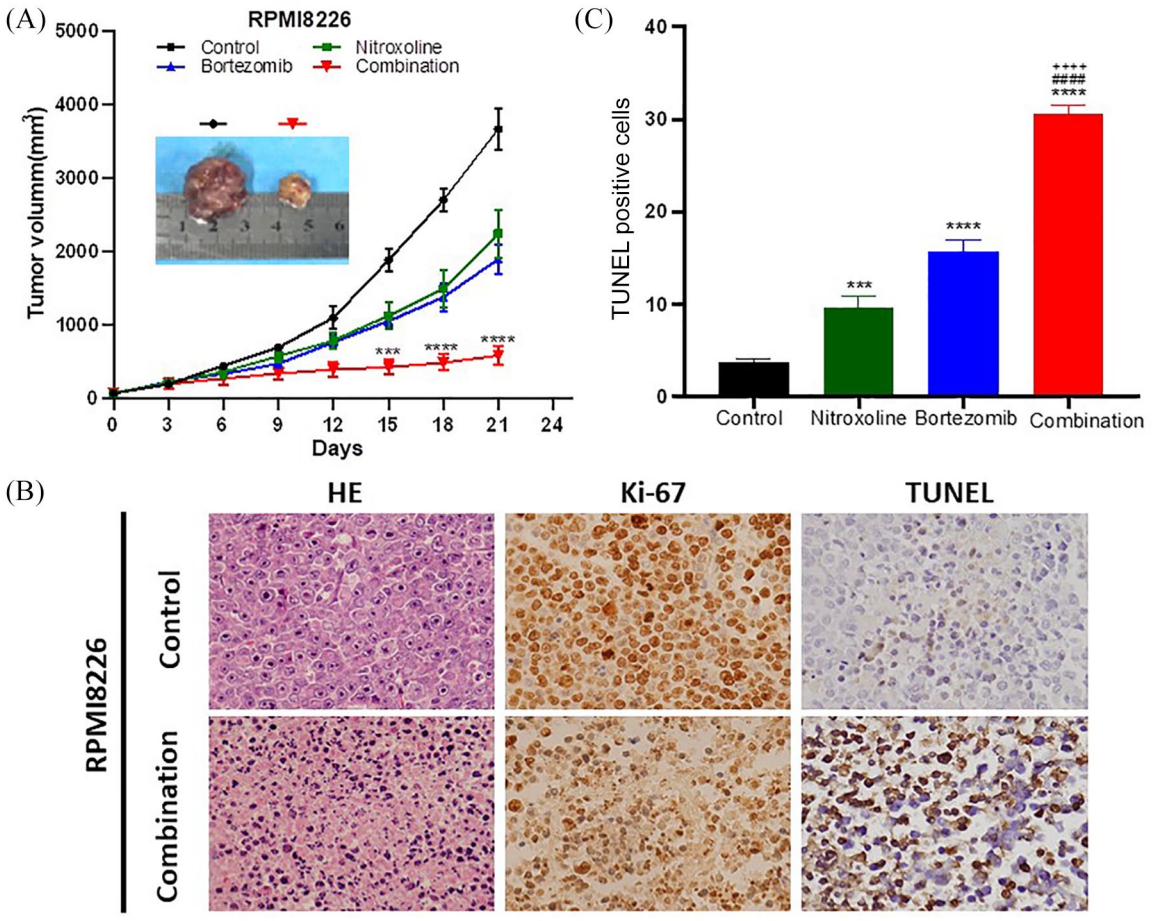

Figure 6. Effects of nitroxoline and bortezomib on tumor growth in an RPMI8226 cell xenograft model *in vivo*. (A) Xenograft tumor volume in mice was measured every 3 days for 21 days. (B) On day 21, mice were euthanized *via* CO2 asphyxiation followed by cervical dislocation to confirm death, and the tumors were excised. Hematoxylin and eosin staining and immunohistochemical staining for Ki-67 expression were performed in the tumor tissue. (C) TUNEL assay for apoptosis in tumor tissues and the average percentage of TUNEL-positive cells per field is reported as mean ± SD. $^{**}p < 0.01$, $^{***}p < 0.001$ and $^{****}p < 0.0001$, *versus* control group; $^{\#\#\#\#}p < 0.0001$ *versus* nitroxoline alone group; $^{++++}p < 0.0001$ *versus* bortezomib alone group.

and nitroxoline in real-world clinical treatment for human MM.

Acknowledgement

Great appreciation should be accorded to all the librarians of Fourth Military Medical University for their kind assistance in literature retrieval.

Author contribution

XQC, YPS and CL conceived the experiment. GL and YHZ drafted the manuscript. GL, YHZ, LX performed the cell experiment and statistical analysis. JF and HLT performed the immunohistochemistry. All authors critically reviewed the manuscript and approved the final version of this manuscript.

Availability of data and materials

Data, samples or materials will be made available upon request by communicating with Xie-Qun Chen.

Conflict of interest statement

The author(s) declare that there is no conflict of interest.

Consent for publication

All authors have read, understood and approved the authorship agreement.

Funding

The author(s) disclosed receipt of the following financial support for the research, authorship,

and/or publication of this article: This study was supported by grants from the National Natural Science Foundation of China 81172247 (to Xie-Qun Chen) and the Natural Science Foundation of Shaanxi Province (grant no. 2017JM8025).

ORCID iD

Yan-Hua Zheng https://orcid.org/0000-0002-7527-8248

References

1. Laubach J, Richardson P and Anderson K. Multiple myeloma. *Annu Rev Med* 2011; 62: 249–264.
2. Zhou L, Jiang H, Du J, *et al.* USP15 inhibits multiple myeloma cell apoptosis through activating a feedback loop with the transcription factor NF-κBp65. *Exp Mol Med* 2018; 50:1–12.
3. Ocio EM, Richardson PG, Rajkumar SV, *et al.* New drugs and novel mechanisms of action in multiple myeloma in 2013: a report from the International Myeloma Working Group (IMWG). *Leukemia* 2014; 28: 525–542.
4. Kumar SK, Rajkumar SV, Dispenzieri A, *et al.* Improved survival in multiple myeloma and the impact of novel therapies. *Blood* 2008; 111: 2516–2520.
5. Kumar SK, Dispenzieri A, Lacy MQ, *et al.* Continued improvement in survival in multiple myeloma: changes in early mortality and outcomes in older patients. *Leukemia* 2014; 28: 1122–1128.
6. Zheng Y, Shen H, Xu L, *et al.* Monoclonal antibodies versus histone deacetylase inhibitors in combination with bortezomib or lenalidomide plus dexamethasone for the treatment of relapsed or refractory multiple myeloma: an indirect-comparison meta-analysis of randomized controlled trials. *J Immunol Res* 2018; 2018: 7646913.
7. Driessen C, Kraus M, Joerger M, *et al.* Treatment with the HIV protease inhibitor nelfinavir triggers the unfolded protein response and may overcome proteasome inhibitor resistance of multiple myeloma in combination with bortezomib: a phase I trial (SAKK 65/08). *Haematologica* 2016; 101: 346–355.
8. Yao Y, Xia D, Bian Y, *et al.* Alantolactone induces G1 phase arrest and apoptosis of multiple myeloma cells and overcomes bortezomib resistance. *Apoptosis* 2015; 20: 1122–1133.
9. Chen R, Yik JHN, Lew QJ, *et al.* Brd4 and HEXIM1: multiple roles in P-TEFb regulation and cancer. *Biomed Res Int* 2014; 2014: 232870.
10. Filippakopoulos P, Qi J, Picaud S, *et al.* Selective inhibition of BET bromodomains. *Nature* 2010; 468: 1067–1073.
11. Rataj O, Haedicke-Jarboui J, Stubenrauch F, *et al.* Brd4 inhibition suppresses HPV16 E6 expression and enhances chemoresponse: a potential new target in cervical cancer therapy. *Int J Cancer* 2019; 144: 2330–2338.
12. Qin A, Li Y, Zhou L, *et al.* Dual PI3K-BRD4 inhibitor SF1126 inhibits colorectal cancer cell growth in vitro and in vivo. *Cell Physiol Biochem* 2019; 52: 758–768.
13. Shen G, Jiang M and Pu J. Dual inhibition of BRD4 and PI3K by SF2523 suppresses human prostate cancer cell growth in vitro and in vivo. *Biochem Biophys Res Commun* 2018; 495: 567–573.
14. Guo N, Zheng J, Zi F, *et al.* I-BET151 suppresses osteoclast formation and inflammatory cytokines secretion by targetting BRD4 in multiple myeloma. *Biosci Rep* 2019; 39: BSR20181245.
15. Jiang H, Xing J, Wang C, *et al.* Discovery of novel BET inhibitors by drug repurposing of nitroxoline and its analogues. *Org Biomol Chem* 2017; 15: 9352–9361.
16. Jung D, Khurana A, Roy D, *et al.* Quinacrine upregulates p21/p27 independent of p53 through autophagy-mediated downregulation of p62-Skp2 axis in ovarian cancer. *Sci Rep* 2018; 8: 2487.
17. Zhang Y, Wang J, Hui B, *et al.* Pristimerin enhances the effect of cisplatin by inhibiting the miR-23a/Akt/GSK3β signaling pathway and suppressing autophagy in lung cancer cells. *Int J Mol Med* 2019; 43: 1382–1394.
18. Pan Y, Gao Y, Chen L, *et al.* Targeting autophagy augments in vitro and in vivo antimyeloma activity of DNA-damaging chemotherapy. *Clin Cancer Res* 2011; 17: 3248–3258.
19. Wang T, Ding Y, Yang Y, *et al.* Synergistic antitumour effects of triptolide plus 10-hydroxycamptothecin onbladder cancer. *Biomed Pharmacother* 2019; 115: 108899.
20. Tsai Y, Lin J, Ma Y, *et al.* Fisetin inhibits cell proliferation through the induction of G(0)/G(1) phase arrest and caspase-3-mediated apoptosis in mouse leukemia cells. *Am J Chin Med* 2019; 47: 841–863.
21. Liu Y, Kang X, Niu G, *et al.* Shikonin induces apoptosis and prosurvival autophagy in human

melanoma A375 cells via ROS-mediated ER stress and p38 pathways. *Artif Cells Nanomed Biotechnol* 2019; 47: 626–635.

22. Hong YS, Hong S, Kim S, *et al.* Bortezomib induces G2-M arrest in human colon cancer cells through ROS-inducible phosphorylation of ATM-CHK1. *Int J Oncol* 2012; 41: 76–82.
23. Brüning A, Burger P, Vogel M, *et al.* Bortezomib treatment of ovarian cancer cells mediates endoplasmic reticulum stress, cell cycle arrest, and apoptosis. *Invest New Drugs* 2009; 27: 543–551.
24. Richardson PG and Anderson KC. Bortezomib: a novel therapy approved for multiple myeloma. *Clin Adv Hematol Oncol* 2003; 1: 596–600.
25. Taylor-Harding B, Agadjanian H, Nassanian H, *et al.* Indole-3-carbinol synergistically sensitises ovarian cancer cells to bortezomib treatment. *Br J Cancer* 2012; 106: 333–343.
26. Pitts TM, Morrow M, Kaufman SA, *et al.* Vorinostat and bortezomib exert synergistic antiproliferative and proapoptotic effects in colon cancer cell models. *Mol Cancer Ther* 2009; 8: 342–349.
27. Jiang L, Wang Y, Zhu F, *et al.* Molecular mechanism of anti-cancer activity of the nano-drug C-PC/CMC-CD59sp NPs in cervical cancer. *J Cancer* 2019; 10: 92–104.
28. Ray A, Jena S, Dash B, *et al.* Hedychium coronarium extract arrests cell cycle progression, induces apoptosis, and impairs migration and invasion in HeLa cervical cancer cells. *Cancer Manag Res* 2019; 11: 483–500.
29. Chen M and Yu S. Lipophilic grape seed proanthocyanidin exerts anti-proliferative and pro-apoptotic effects on PC3 human prostate cancer cells and suppresses PC3 xenograft tumor growth in vivo. *J Agric Food Chem* 2019; 67: 229–235.
30. Ye G, Kan S, Chen J, *et al.* Puerarin in inducing apoptosis of bladder cancer cells through inhibiting SIRT1/p53 pathway. *Oncol Lett* 2019; 17: 195–200.
31. Guo J, Han T, Bao L, *et al.* Ursolic acid promotes the apoptosis of cervical cancer cells by regulating endoplasmic reticulum stress. *J Obstet Gynaecol Res* 2019; 45: 877–881.
32. Zhang Y, Bai C, Lu D, *et al.* Endoplasmic reticulum stress and autophagy participate in apoptosis induced by bortezomib in cervical cancer cells. *Biotechnol Lett* 2016; 38: 357–365.
33. Liu X, Jiang Q, Liu H, *et al.* Vitexin induces apoptosis through mitochondrial pathway and PI3K/Akt/mTOR signaling in human non-small cell lung cancer A549 cells. *Biol Res* 2019; 52: 7.
34. Wang J, Li H, Wang X, *et al.* Alisol B-23-acetate, a tetracyclic triterpenoid isolated from Alisma orientale, induces apoptosis in human lung cancer cells via the mitochondrial pathway. *Biochem Biophys Res Commun* 2018; 505: 1015–1021.
35. Zheng G, Ji H, Zhang S, *et al.* Selenious-β-lactoglobulin induces the apoptosis of human lung cancer A549 cells via an intrinsic mitochondrial pathway. *Cytotechnology* 2018; 70: 1551–1563.
36. Zhang Y, Zhang XX, Yuan RY, *et al.* Cordycepin induces apoptosis in human pancreatic cancer cells via the mitochondrial-mediated intrinsic pathway and suppresses tumor growth in vivo. *Onco Targets Ther* 2018; 11: 4479–4490.
37. Zhang M, Du H, Huang Z, *et al.* Thymoquinone induces apoptosis in bladder cancer cell via endoplasmic reticulum stress-dependent mitochondrial pathway. *Chem Biol Interact* 2018; 292: 65–75.
38. Wu D, Zhao Y, Fu S, *et al.* Seleno-short-chain chitosan induces apoptosis in human breast cancer cells through mitochondrial apoptosis pathway in vitro. *Cell Cycle* 2018; 17: 1579–1590.
39. Mortenson MM, Schlieman MG, Virudachalam S, *et al.* Reduction in BCL-2 levels by 26S proteasome inhibition with bortezomib is associated with induction of apoptosis in small cell lung cancer. *Lung Cancer* 2005; 49: 163–170.
40. Bergogne-Berezin E, Berthelot G and Muller-Serieys C. [Present status of nitroxoline]. *Pathol Biol* 1987; 35: 873–878.
41. Huang SY, Chang CS, Liu TC, *et al.* Pharmacokinetic study of bortezomib administered intravenously in Taiwanese patients with multiple myeloma. *Hematol Oncol* 2018; 36: 238–244.